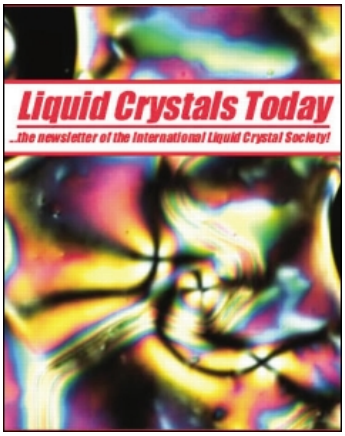

Liquid Crystals Today
Publication details, including instructions for authors and subscription information:
http://www.informaworld.com/smpp/title~content=t713681230

Optical manipulation and self-assembly of nematic colloids: colloidal crystals and superstructures

Igor Muševič[ab]
[a] J. Stefan Institute, Ljubljana, Slovenia [b] Faculty of Mathematics and Physics, University of Ljubljana, Ljubljana, Slovenia

Online publication date: 15 June 2010

To cite this Article Muševič, Igor(2010) 'Optical manipulation and self-assembly of nematic colloids: colloidal crystals and superstructures', Liquid Crystals Today, 19: 1, 2 — 12
To link to this Article: DOI: 10.1080/13583140903395947
URL: http://dx.doi.org/10.1080/13583140903395947

Liquid Crystals Today
Vol. 19, No. 1, June 2010, 2–12

Taylor & Francis
Taylor & Francis Group

RESEARCH ARTICLE

Optical manipulation and self-assembly of nematic colloids: colloidal crystals and superstructures

Igor Muševič*

J. Stefan Institute, Jamova 39, 1000 Ljubljana, Slovenia; Faculty of Mathematics and Physics, University of Ljubljana, Jadranska 19, 1000 Ljubljana, Slovenia

(*Received 14 April 2009; final version received 12 May 2009*)

Optical manipulation of colloidal particles in nematic liquid crystals is far more complex than manipulation in water-based colloids. Owing to the long-range nature of the orientational ordering, their elasticity and topological conservation laws, almost any kind of object can be trapped and manipulated in liquid crystals. Furthermore, local heating due to the absorption of light can be used to create microdroplets of the isotropic phase, which interact strongly with colloidal particles. This leads to a broad variety of colloidal assemblies in liquid crystals, which cannot be observed in isotropic solvents: colloidal wires, assembled by entangled topological defects, superstructures in mixtures of large and small colloidal particles and a broad variety of two-dimensional nematic colloidal crystals. In all cases, the colloidal binding energy is several orders of magnitude stronger compared with water-based colloids. The large variety of colloidal superstructures, which can be assembled in nematic colloids, makes them highly interesting for application in photonic materials.

Keywords: nematic liquid crystal; colloids; laser tweezers; manipulation; colloidal crystals; colloidal superstructures

1. Introduction to nematic colloids

One of the central issues of the 'bottom-up' approach in nanotechnology is the ability to control regular spatial arrangements of particles in space. Many different approaches have been developed to date, and their applicability ranges from nanoscale to micrometre-scale systems and devices. On a mesoscopic scale, methods of sub-micrometre particle manipulation have been developed, using laser tweezers or optoelectronic tweezers (*1, 2*), microfluidics (*3*), optofluidics (*4*), micromanipulation (*5*), and growth on patterned surfaces (*6*). Of particular interest is directed-assembly and self-assembly of colloidal particles in pre-determined colloidal structures, such as two-dimensional and three-dimensional photonic crystals (*7, 8*) or metamaterials (*9, 10*). Although several interesting self-assembly concepts have been demonstrated, they all suffer from a major limitation, which is the difficulty of scaling-up from the nanoscale to real device dimensions. Most of the concepts rely on particle manipulation using electromagnetic forces, such as van der Waals and screened electrostatic forces in a water environment. These forces are very difficult to control over macroscopic length scales, are very sensitive to conditions at the surfaces of interacting particles and depend on the properties of the medium where the particles are dispersed, which is usually water. Scientists have been attempting for a long time to develop a technology for self-assembling three-dimensional photonic crystals from water-based colloidal systems, using sedimentation from colloidal dispersions, growth on patterned surfaces and external assisted manipulation. Many impressive fundamental results have emerged from these studies, but, despite enormous efforts, the problem of controlled growth of microcolloidal structures from water-based colloidal systems has remained mostly unsolved (*11*). Novel approaches using novel forces and conceptually novel solutions are needed. In recent years, several conceptually novel approaches to colloidal self-assembly have emerged, which are related to the properties of the matter carrying the colloidal particle interactions. For example, two such approaches are: (1) using structural forces in nematic liquid crystal colloids to control the spatial arrangement and binding of particles (*12, 13*); (2) using the magnetic properties of colloids and carrying fluid to assemble colloidal superstructures has been demonstrated recently in dispersions of paramagnetic and diamagnetic colloidal particles in magnetic ferrofluids (*14*). Owing to the limited space available, it is not possible to mention here all the valuable achievements in the rapidly growing field of nematic colloids. Instead, the aim of this paper is to present in simple words the main ideas and state-of-the-art in the field of nematic colloids with an emphasis on the work performed by my group.

To my knowledge, the forces between particles in the nematic liquid crystal were first observed in the 1970s (*15, 16*) and were used efficiently to 'decorate'

*Email: igor.musevic@ijs.si

ISSN 1358-314X print/ISSN 1464-5181 online

DOI: 10.1080/13583140903395947
http://www.informaworld.com

and visualise the orientation of liquid crystalline molecules at the surface of a nematic liquid crystal. In those early experiments, it was observed that small bubbles organise in chains at the free surface of a nematic liquid crystal (see Figure 4.4. in de Gennes and Prost (*16*)), and the chains follow the overall orientation of the nematic. Whereas in those experiments the effects of surface tension certainly influenced the self-organisation of particles at the nematic-air interface, these effects were eliminated in the work of Poulin *et al.* (*12, 13*) on nematic emulsions. In the nematic liquid crystal, they observed the spontaneous organisation of small droplets of water in chains, which did not coalesce. This was clear evidence of a novel type of force between inclusions in the nematic liquid crystal, called structural forces, and also an indication of a new conservation law for a new physical quantity, that is, topological charge. Whereas van der Waals and electrostatic forces between bodies are mediated by the electromagnetic field and can be transmitted either across a vacuum or matter, structural forces in liquid crystals are mediated by the orientational order of the liquid crystal and can be transmitted only in a liquid crystal. We can, therefore, consider the electromagnetic field to have been substituted by the orientational field, describing the order in liquid crystals. This is a tensorial field and the phenomena emerging from it are expected to be far more complex than phenomena of electromagnetic origin.

It should be noted that the structural forces between the particles in liquid crystals are a consequence of change in the free energy of the nematic liquid crystal. A general definition of the force has to be considered here, which reads: when the total free energy F of the system depends on the separation s between the two particles, the force F is generated, which is the separation derivative of the free energy, $F = -\partial \mathrm{F}/\partial s$. It is therefore, a generalised force, which is of thermodynamic origin, and it is evident that both the change of entropy of a liquid crystal (which is related to the degree of order), and the energy change, which is due to elastic distortion of the nematic, have to be considered. In principle, the contribution of fluctuations in the tensorial field also have to be considered, which would lead to the Casimir effect in liquid crystals (*17*). For simplicity, these fluctuation effects are ignored and only the mean-field forces are dealt with here. In addition, the fully tensorial Landau–de Gennes theory for the description of structural forces in liquid crystals has to be used because we are inevitably dealing with various forms of topological defects, where the degree of order changes significantly in the core of the defects.

2. Topological dipoles and quadrupoles

When a small colloidal particle, such as one of the silica microspheres shown in Figure 1, is immersed in the nematic liquid crystal, the surface of the particle interacts with the liquid crystalline molecules and forces them to align into a preferred direction relative to the surface. This surface-induced order creates distortion of the nematic around the particle, which spreads over macroscopic distances. It can also be seen from Figure 1(b) that the particle is accompanied by a dark spot, which makes the distortion of the liquid crystal around the microsphere non-spherical, even though the particle itself is spherical. This dark spot is a point hyperbolic hedgehog defect (*18*), which appears dark because the director field around the defect is highly curved and inhomogeneous. The spatial inhomogeneity of orientation gives rise to a strong local variation of birefringence and results in a strong scattering of light. The appearance of the defect is inevitable due to the conservation law for topological charge, and for the same reason, the defect cannot be separated from the particle (*18*). The point defect and the colloidal particle form a 'topological' dipole (*12, 13, 19–23*). The mathematical description of the interactions between colloidal particles in the nematic crystals is in fact very similar to the electrostatic interaction between the electric charges (*13, 18*), but this simple electrostatic picture breaks-down in some important cases (*24*). The corresponding director field around the topological dipole is illustrated in Figure 1(c).

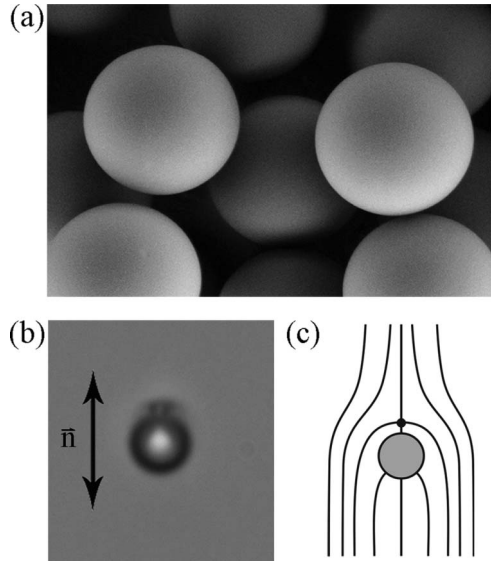

Figure 1. (a) Scanning electron microscopy image of micrometre-sized silica microspheres. (b) A silica microsphere with homeotropic surface anchoring in a planar cell filled with 4-cyano-4-n-pentylbiphenyl. A hedgehog point defect is visible. (c) Sketch of 'dipolar' director field around the microsphere with the homeotropic surface anchoring in a planar cell. The arrow indicates the orientation of the nematic far away from the particle.

Figure 2 shows another possible director configuration, which is of quadrupolar symmetry and a thin defect ring encircles the particle at its equator (*25–32*). Such a quadrupolar colloidal particle can be obtained using an appropriate surface preparation technique or adjusting the size of the particle. Whether a given colloidal particle appears as a dipolar or quadrupolar particle depends on its size, surface preparation and the thickness of the cell where the dispersion of particles was prepared. For a given radius R and the surface preparation of the particle, there is a critical thickness h_c of the cell, which determines the transition from the dipolar to the quadrupolar type (*18*). Such a situation is shown in Figure 3, where glass microspheres with homeotropic surface anchoring were dispersed in 4-cyano-4-n-pentylbiphenyl (5CB) and introduced into a wedge-type cell with variable thickness. The surfaces of the confining cell were prepared so as to induce a strong planar alignment of 5CB, which has a strong influence on the director distribution around colloidal particles when the gap is comparable to the diameter of the particles. For $h > h_c$, the influence of the wall is small and colloidal particles are of dipolar symmetry, whereas for $h < h_c$, the confinement walls induce quadrupolar symmetry of the nematic liquid crystal around the colloidal particle.

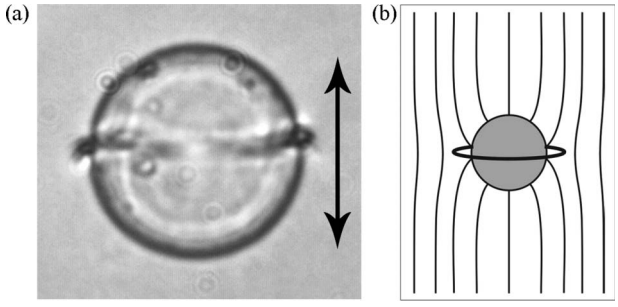

Figure 2. (a) Microscope image of a Saturn ring defect around a 20 μm diameter glass microsphere with homeotropic surface anchoring of 4-cyano-4-n-pentylbiphenyl. (b) Schematic drawing of the director field around the colloidal particle.

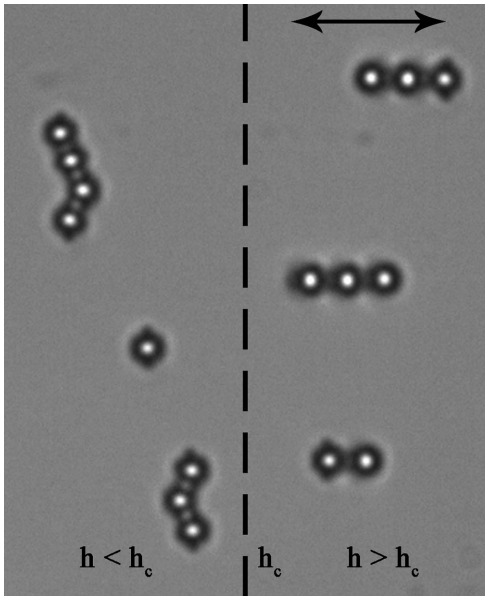

Figure 3. In a wedge-type planar cell with variable thickness, the region of critical thickness h_c is observed. Dipoles exist at larger thickness, $h > h_c$, Saturns at lower thickness, $h < h_c$.

3. Manipulation of colloidal particles in the nematic liquid crystal by laser tweezers

If the forces between two or many micrometre-sized colloidal particles in a nematic liquid crystal are to be studied and measured, an appropriate tool has to be used for grabbing and manipulating individual microparticles. An elegant solution to this problem is to use laser tweezers, as it is well known since the optical levitation experiments of Ashkin (*33*) that micron-sized transparent particles can be trapped by strongly focused laser light. However, there is a very important limitation in that the refractive index of the particles is higher than that of the surroundings. The effect is extensively used in optical tweezers to trap, manipulate and sort particles with light (*34*). One of the serious limitations of laser tweezers, therefore, is the necessity for particles to have a refractive index larger than that of the surroundings. As the indices of a typical liquid crystal are relatively high (ordinary index of 1.5 and extraordinary index around 1.7), this seems to reduce possible choices for colloidal materials. Laser tweezers were used to trap and measure forces between polystyrene colloids ($n = 1.59$) in low-index nematic liquid crystals (*35–39*), to switch liquid crystal microdroplets (*40, 41*), to manipulate defects in lyotropic liquid crystals (*42*), to manipulate islands on freely suspended smectic films (*43*), to trap and manipulate high-index colloids in the nematic (*44*) and defects in a nematic liquid crystal (*45*).

An unusual mechanism of laser trapping and manipulation of nematic colloids has been reported (*46, 47*). In those experiments, micron-sized glass particles (refractive index $n = 1.44$) with homeotropic boundary conditions were dispersed in the nematic liquid crystal with refractive indices $n_\circ = 1.52$ and $n_e = 1.74$ that were both larger compared with the refractive index of colloidal particles. Under such conditions, a repulsive force is expected to arise between the waist of a strongly focused light and the colloidal particle. Surprisingly, the opposite was clearly observed, that is, the low-index colloidal particle was

attracted into the laser focus over extraordinarily large separations of several micrometres.

Three different mechanisms have been identified (*47*), which lead to this 'forbidden trapping', and they depend on the intensity of the trapping light and, in extreme cases, on the absorption and local melting of a liquid crystal. The important threshold is the intensity, where the optical Freedericksz transition (OFT) occurs in a liquid crystal cell with given material and geometrical parameters. In the optical Fredericksz transition, the electric field of the electromagnetic wave forces the molecules to align in the field direction via the difference of the dielectric constant for optical frequencies, that is, via the birefringence of the liquid crystal material.

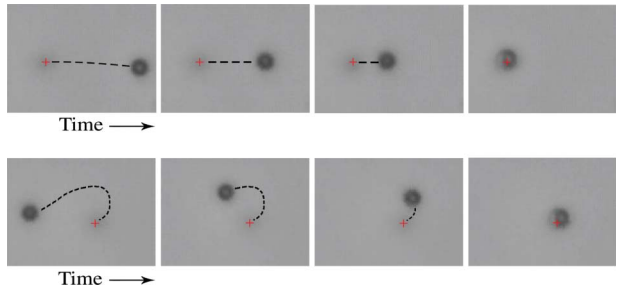

Figure 4. Time sequences of microscopic images showing trapping trajectories of a low-index 1 μm diameter colloidal particle with homeotropic surface anchoring in a homeotropic cell of 4-cyano-4-n-pentylbiphenyl. The focus of the laser tweezers is indicated by the red cross and is visible because the light intensity is above the optical Freedericksz transition and the nematic is distorted.

(1) Well below the OFT, the optical trapping of low-index colloidal particles in a high-index nematic is sensitive to the polarisation of the trapping beam. The surface-induced distortion of the director field around the colloidal particle is accompanied by spatially varying direction of the eigenaxis of the dielectric tensor for optical frequencies. For a particular polarisation of the trapping beam, there are two energetically favourable locations of the beam waist, where the polarisation is directed along the long axis of the molecules and the electromagnetic energy is minimised. Owing to the gradient of the free energy, the colloid is attracted into the laser focus until the favourable region of the distorted director field is in the most intense part of the optical trap.

(2) Above the OFT threshold, highly localised light intensity induces local rotation of molecules into the field direction and creates a localised region of elastic distortion in the liquid crystal. This distorted region can itself be considered as a virtual colloidal particle, which interacts with the real colloidal particle in its vicinity. The mechanism of optical trapping is, therefore, accompanied by the elasticity-mediated interaction between two objects; the first object being the optically distorted region of a liquid crystal and the second object being the colloidal particle. The trapping mechanism is highly anisotropic and the trajectories of the particles could be quite complex, as illustrated in Figure 4.

(3) When the absorption of laser light is very high, the nematic liquid crystal can be locally molten by the laser tweezers. This creates a small isotropic island of controlled size in the nematic phase, which can be moved around and behaves as a colloidal particle, interacting with real colloidal particles. Owing to its isotropic–nematic surface tension, this isotropic droplet interacts strongly with colloidal particles and can be used as an efficient tool to assemble colloidal structures.

In experiments on nematic colloids, it is observed that practically any kind of object could be trapped and manipulated with laser tweezers in the nematic liquid crystal, irrespective of its refractive index. This greatly facilitates the choice of materials that can be used in nematic colloidal dispersions.

Laser tweezers are not only a convenient tool with which to assemble artificial nematic colloidal structures by manipulating individual particles and thus driving directed colloidal assembly, but can be used together with an optical particle tracking technique to study the structural forces between objects in liquid crystals. The technique is simple and the separation-dependence of the force between two particles can be determined using ordinary optical video-capturing microscopy (*46–48*). Briefly, the force $F_{colloid}(\vec{r})$ on a colloidal particle in the nematic liquid crystal is determined by monitoring the movement of the centre of gravity of that particle and recording its trajectory $\vec{r}(t)$. The centre of gravity of the particle can be determined with great precision (down to ± 2 nm) graphically. As the motion of particles in the nematic liquid crystal is highly damped by the viscosity η of the liquid crystal, the resulting acceleration $\vec{a}$ in Newton's law of motion is practically zero, $\vec{F} = \vec{F}_{colloid} + \vec{F}_{drag} = m \cdot \vec{a} \approx 0$. This means that the force on the colloidal particle $\vec{F}_{colloid}(\vec{r})$ is at all times practically equal to the viscous drag force, which, for a spherical object, is equal to the Stokes force, $\vec{F}_{drag} = 6\pi R\eta\vec{v} = 6\pi R\eta d\vec{r}/dt$. The velocity of the particle $\vec{v}(r)$is determined by numerically differentiating the recorded trajectory of the particle, $\vec{v}(\vec{r}) = d\vec{r}/dt$, and the drag coefficient $6\pi R\eta$ can be determined directly from a

separate experiment, where the Brownian motion of the particle is recorded (*48*). From the calculated force on the colloidal particle as a function of separation, the potential energy $U(\vec{r})$ of a particle due to its elastic interaction with another object is obtained by numerical integration, $U(\vec{r}) = \int_{\infty}^{r} \vec{F}_{colloid}(s)d\vec{s}$. The method of determining the interaction energy of a pair of colloidal particles in the liquid crystal therefore is simple and accurate, and different pair-interaction potentials can be measured by just bringing two colloidal particles into close vicinity using laser tweezers, releasing them and capturing a video of their movement.

4. Dipolar, quadrupolar and mixed interactions in nematic colloids

When several colloidal particles are brought together in the nematic liquid crystal, their regions of distortion, which spread out over several micrometres, start to overlap. This generates structural forces between the particles, which are anisotropic, very strong and of long range. Typically, two micrometre-size colloidal particles in a thick nematic liquid crystal cell will 'feel' each other at a separation of 10 μm, which results in fascinating self-assembling behaviour. It has been shown that these long-range forces lead to a diversity of self-assembled structures, such as linear chains of colloidal particles (*13, 23*), anisotropic clusters (*49*), regular defect arrays (*35*), two-dimensional hexagonal and dense colloidal lattices at interfaces (*50, 52*), particle-stabilised defect gels (*51*), cellular soft-materials (*53, 54*) and two-dimensional colloidal crystals in thin nematic cells (*55*).

Figure 5 shows two simple examples of linear colloidal objects assembled from nematic colloids.

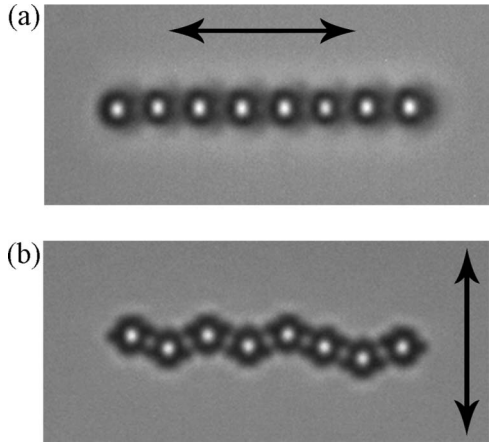

Figure 5. (a) Chain of dipolar colloidal particles in a planar cell of 4-cyano-4-n-pentylbiphenyl. (b) Quadrupolar chain is always kinked.

Figure 5(a) shows a straight chain, assembled from dipolar nematic colloids, which are observed in thicker planar nematic cells (*56*), whereas chains from quadrupolar nematic colloids in thinner cells are kinked (*57*), as shown in Figure 5(b). These two examples clearly show the anisotropic nature of the structural forces in nematic colloids, as the colloidal chaining cannot be observed in isotropic solvents, such as water.

The mechanism of such anisotropic interactions is simple: each colloidal particle is surrounded by the elastically distorted region of a nematic liquid crystal, which is non-spherical due to topological conservation laws and the presence of defects (*18, 25*). For two dipolar colloidal particles, the total elastic energy is lowered if they share the regions of similar distortion. This is the reason why two collinear colloidal dipoles will be attracted in a head-to-tail manner, similar to the interaction of two collinear electric dipoles.

Figure 6 illustrates two possible scenarios of pair attraction of dipolar nematic colloids, where the topological dipole of each particle points either along or against the nematic director far away from the particles. Two collinear dipoles will attract if their dipoles are pointing in the same direction (Figure 6(a)), and will be repelled if their dipoles are antiparallel. However, the opposite happens if the two dipoles are positioned side-by-side: they are repelled if their dipoles are parallel and are attracted if their dipoles are antiparallel (Figure 6(b)). Figure 7 shows a typical separation-dependence of the attractive potential between two collinear dipolar colloidal particles in the nematic liquid crystal 5CB. The attractive potential is long range and very strong, reaching values of several $1000k_BT$ for micrometre-sized colloidal particles and surface-to-surface separations of several hundreds of nanometres. Similar to the electrostatic interaction between two permanent electric dipoles,

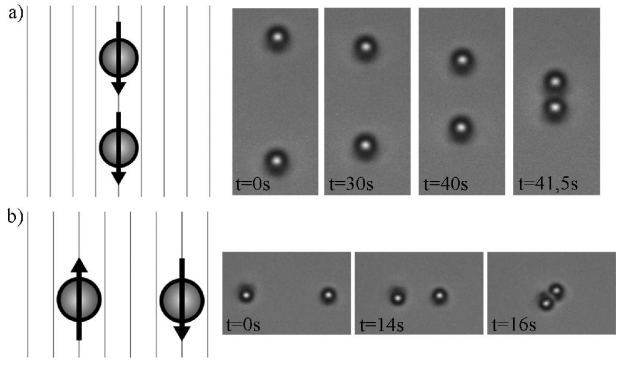

Figure 6. Attraction of topological dipoles-microspheres with homeotropic surface anchoring of 4-cyano-4-n-pentylbiphenyl in a planar cell. Note the similarity with electric dipoles.

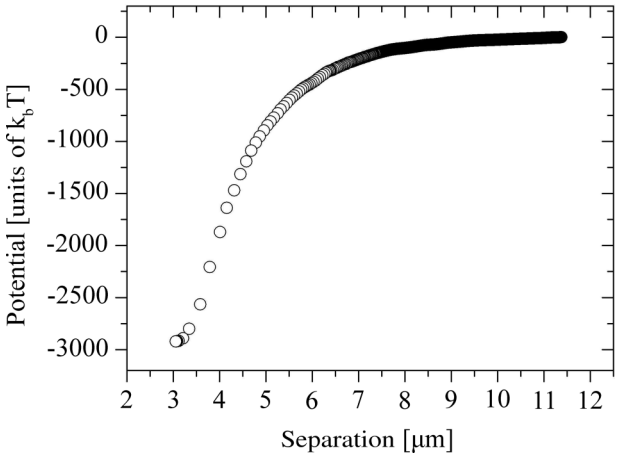

Figure 7. Interaction potential between two dipolar colloidal particles in a planar cell of 4-cyano-4-n-pentylbiphenyl nematic liquid crystal. The diameter of the particles is 2.3 μm and their surfaces induce homeotropic surface alignment of 4-cyano-4-n-pentylbiphenyl.

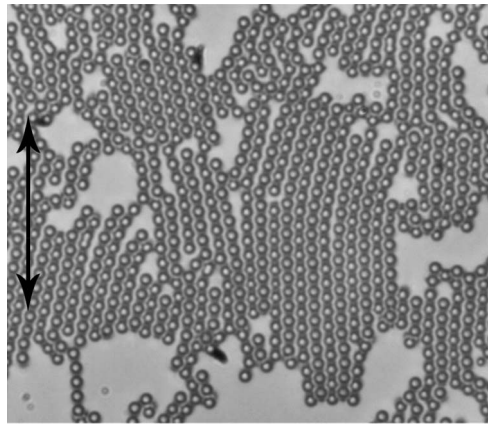

Figure 8. Dipolar nematic colloids in a planar cell of 4-cyano-4-n-pentylbiphenyl. The thickness of the cell is smaller than twice the diameter of the particles. The concentration of microspheres has been increased so that densely packed structures are observed.

the structural force between two dipolar colloidal particles shows $1/r^4$ power law dependence, where r is the dipole-dipole separation (*36, 39, 56, 58–60*). Forces between two quadrupolar colloidal particles are also of long range, but the strength of interaction is nearly one order of magnitude lower (*38, 57, 61*). Recently, it has been found that mixed interactions are also observed in a mixture of topological dipoles and quadrupoles. Here, a selected topological dipole will interact with another quadrupolar particle through a very anisotropic pair potential. This dipole-quadrupole interaction is strong and very anisotropic (*62*).

5. Two-dimensional nematic colloidal crystals

One-dimensional self-organisation of colloidal particles in straight chains of dipolar colloidal particles and kinked chains of quadrupolar colloidal particles are usually observed in cells filled with nematic colloidal dispersion at a small concentration of colloidal particles. When the particle concentration is increased, and the thickness of the cell is still small enough to prevent the formation of multiple layers of colloidal particles, one can observe the spontaneous formation of quasi-ordered regular two-dimensional structures, as shown in Figure 8. Interesting features could be observed from careful inspection of the quasi-ordered regions and it seems they are formed by spontaneously formed series of parallel dipolar chains. The long-range order is disrupted by localised defects, which are inevitably formed in prepared cells. It is clear therefore that some sort of directed-assembly is necessary to produce well-ordered colloidal crystals.

In order to understand the rather complex process of self-assembly of dipolar colloids into two-dimensional crystals, the process of formation was studied in steps. In each step, the forces, which led the particles to organise in ordered structures, similar to electrostatics, were investigated. The force between a single dipolar colloidal particle and a dipolar cluster was analysed first, shown in Figure 9 (*55, 56*). Figure 9(a) shows the interaction of a dipolar colloidal particle with the dipolar cluster, where the topological dipole of the particle and those of the particles in the first neighbouring chain of the cluster point in the same direction.

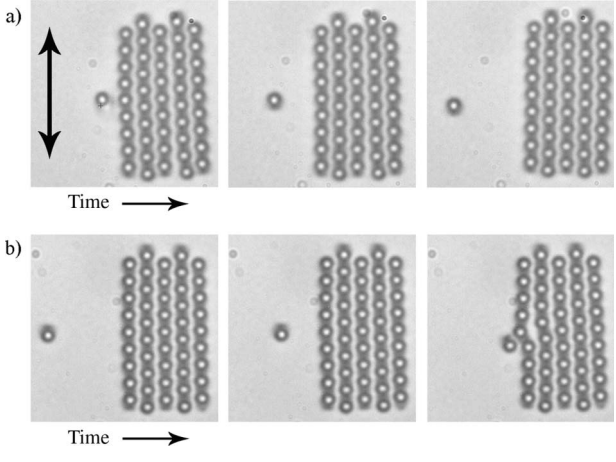

Figure 9. (a) Repulsion between a dipolar colloidal particle and a small dipolar crystal. Note the orientation of the particle's topological dipole with respect to the dipoles in the first-neighbouring chain of the crystallite. (b) When the direction of the particle's dipole is reversed, it is strongly attracted to the first chain in the crystallite.

The repulsive force is clearly visible and the particle is strongly repelled from the first chain. The opposite is observed for the antiparallel orientation of the dipoles, as shown in Figure 9(b): the antiparallel dipolar colloidal particle is strongly attracted to and almost incorporated into the dipolar chain, which illustrates very strong attraction. This is an important finding, as we can conjecture that following the same reason, two dipolar chains with antiparallel topological dipole moments should attract, whereas chains with parallel dipole moments should repel. This was indeed observed in the experiments. Figure 10 shows a strong attraction between two dipolar colloidal chains with antiparallel dipoles, where the binding energy is as high as $10.000k_BT$ for a pair of dipolar chains containing six particles each. Following the same principle, using laser tweezers, a large area of two-dimensional dipolar nematic colloidal crystals can be built, as the one shown in Figure 11(a) (*55*).

In addition to two-dimensional dipolar nematic colloidal crystals, a quadrupolar crystal can be assembled in thinner cells (*55, 57*), which is shown in Figure 11(b). Moreover, it has been reported recently that a whole new class of 'binary' nematic colloidal crystals could be assembled in cells where the dipolar and quadrupolar types of nematic colloids coexist (*62*). This can be achieved in the range of thickness of the cell, which is close to the critical thickness h_c Two different two-dimensional crystalline structures have been reported so far, which are shown in Figure 11(c) and (d), but there are in fact many different possible two-dimensional binary crystals. As many as 12 different binary crystals have been successfully assembled so far and this will be reported elsewhere.

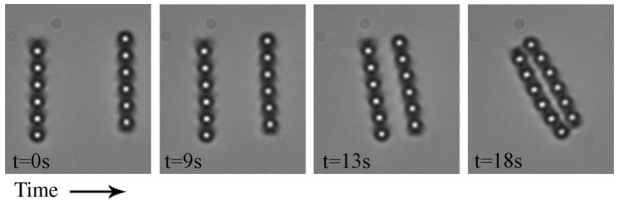

Figure 10. Attraction of two dipolar chains with antiparallel topological dipoles. The dipoles in the left chain are pointing upwards, the dipoles in the right chain point downwards, as is evident from the dark spots, which are hedgehog point defects.

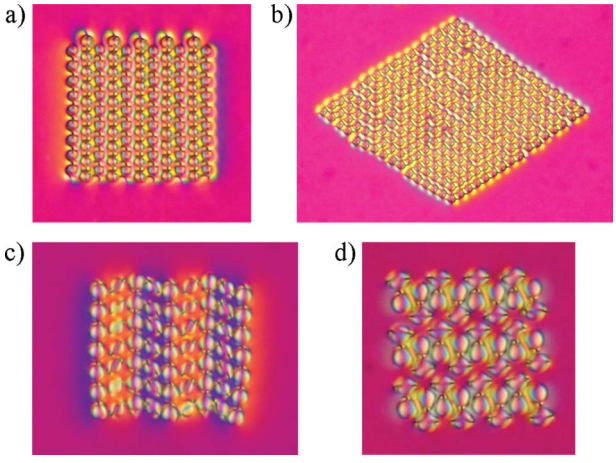

Figure 11. (a) Dipolar nematic colloidal crystal. (b) Quadrupolar nematic colloidal crystal. (c) and (d) Two different binary nematic colloidal crystals assembled from dipoles and quadrupoles.

6. Entanglement of nematic colloids

It has been predicted that colloidal particles could be assembled in nematics with another sort of defect, which is delocalised, and form defect lines (*63–65*). This has been proven in laser tweezer experiments and Landau-de Gennes analysis (*66*), where a liquid crystal was heated locally into the isotropic phase using a high-powered laser beam of laser tweezers, so that an island of the isotropic phase was formed, surrounded by the nematic, as shown in Figure 12. After switching off the

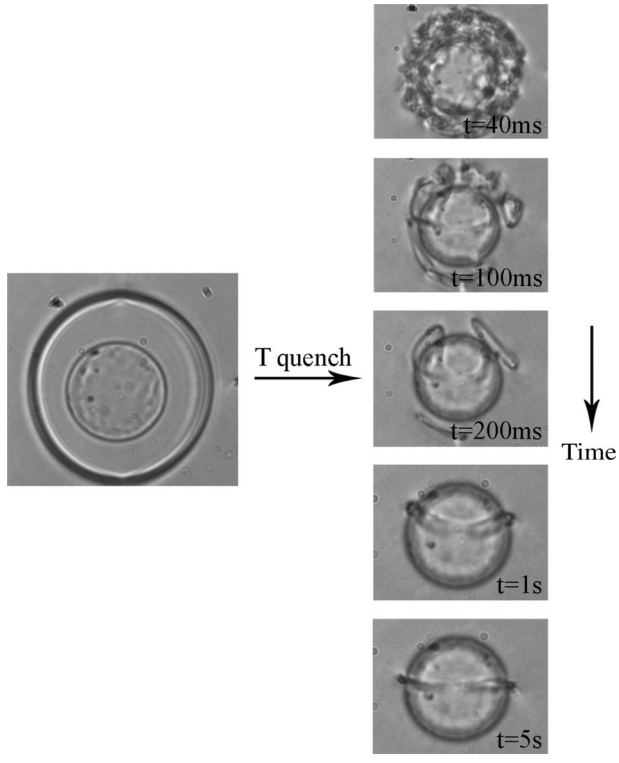

Figure 12. (a) Using heating by laser tweezers, an island of isotropic phase is formed around a colloidal particle. After the light is switched off, a dense tangle of defects is formed, which evolves into a single Saturn ring encircling the particle.

light, the isotropic phase was quenched into the nematic phase, which created a dense tangle of defect lines. In the course of time the lines were annihilated, transforming the defect tangle into a well-orientated nematic and finally a single Saturn ring remained, encircling the colloidal particle. The ring remains because of the conservation of the topological charge, and the experimental conditions were selected so that the quadrupolar colloids are stable.

When this experiment is performed on two colloidal particles, the outcomes can be quite diverse (*66*). In most cases, isolated Saturn rings are formed around individual particles but in some cases, defect rings, entangling both particles, are observed, as shown in Figure 13. The figure presents the time sequence of unpolarised optical micrographs of the time-evolution of a defect tangle in the nematic liquid crystal around two 19 μm colloidal particles after quenching. The formation of a single disclination loop can clearly be seen, formed after switching off the light. In less than 1 s, the 'entangled topological defect' was created, encircling both particles in a form of a twisted loop, a 'figure of eight'.

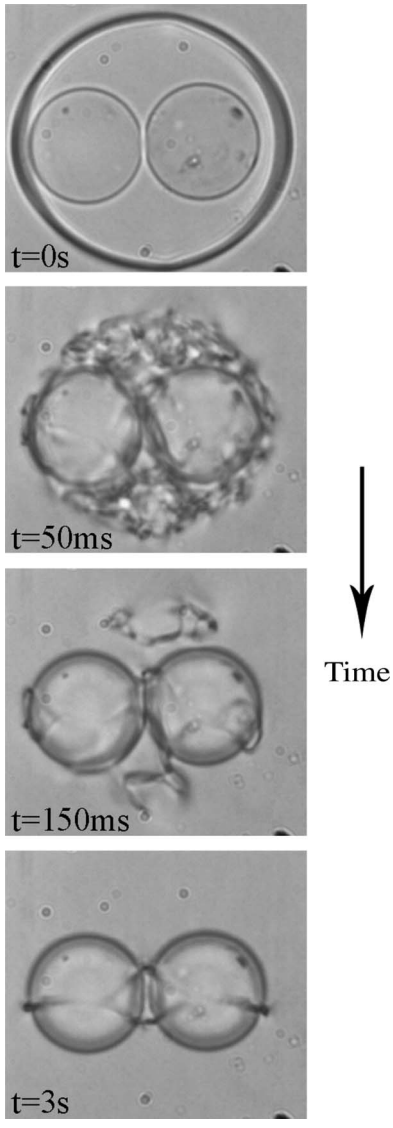

Figure 13. Formation of the 'figure of 8' defect line, which is a single closed defect loop encircling both colloidal particles.

Figure 14(a) presents the formation of a more complicated asymmetric entangled defect loop, which is called the 'figure of omega'. In contrast to the figure of eight, the figure of omega has a straight line at the front, which sinks behind both colloidal particles and makes an additional loop in between them. In most of the experiments, this configuration was unstable and transformed slowly into another stable configuration, shown in Figure 14(b). Here, the final separation between the surfaces of 19 μm spheres was around 4.1 μm, which indicates the presence of a large object in between the spheres. The numerical calculations suggest that the structure is formed by two orthogonal defect rings, each being equivalent to the hyperbolic hedgehog with a topological charge 1. The hidden massive point between both spheres in Figure 14(b) is in fact a small ring (or point defect), situated between the colloidal particles and surrounded by a defect loop encircling both particles. It is called it the 'entangled hyperbolic defect'

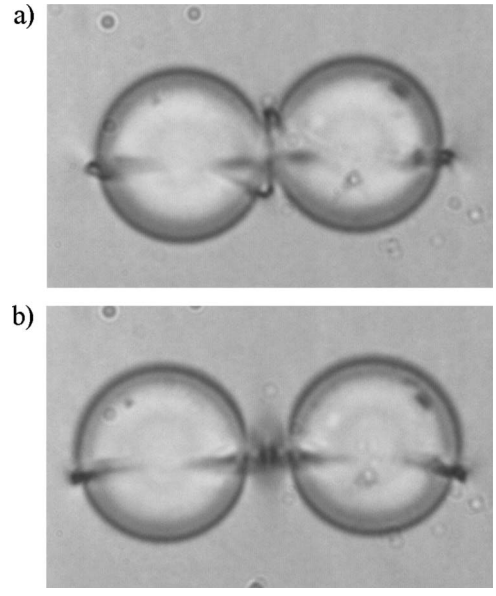

Figure 14. (a) 'Figure of omega' defect line, which is a single twisted line entangling both colloidal particles. In our experiments, this configuration is metastable and transforms into (b), which is the 'entangled point defect' configuration.

structure. The entanglement is not necessarily limited to colloidal pairs, but can extend over many colloidal particles forming colloidal wires.

The strength of the entanglement can be measured using laser tweezers with two separated light traps. Using these traps, two microspheres are grabbed by separate light traps and displaced into opposite directions. After the light is switched off, the defect loop acts as a string, pulling both colloidal particles together. From the recorded images, the effective force and binding potential of the entangled line defects can be determined as a function of separation. At larger separations, the force is string-like and corresponds roughly to the nematic deformation energy per unit length of disclination line. It yields extremely strong effective inter-colloidal interaction, that is, of the order of $10{,}000k_BT$ for 4.7 μm microspheres.

7. Hierarchical colloidal superstructures

The experiments and theory suggest that, in principle, a sophisticated scaffold of topological defect loops can be created in nematic colloids. These are characterised by a reduced nematic order parameter, S, in the core of the defect loops, as well as a highly distorted nematic director in the vicinity of defect lines. It is reasonable to consider that a small colloidal particle in the vicinity of the defect line, which also disturbs the local nematic order, will interact with the defects. It may, therefore, be more favourable energetically for the smaller colloidal particle to migrate into the core of the defect, which minimises the total free energy by sharing the region of distortion and disorder (*67–69*). The driving force for particle migration is, therefore, of an entropic and elastic origin. Recent experiments indeed confirmed this scenario (*68, 70*), and some experimental realisations are shown in Figure 15(a)–(c). Figure 15(a) is a microscope image of a 19 μm colloidal particle with a Saturn ring around it, which is filled with smaller and larger colloidal particles, thus creating a kind of colloidal necklace. Smaller colloidal particles are also strongly attracted to the entangled loops of the figure of eight, which is shown in Figure 15(b) and (c).

The observed colloidal superstructures in the nematic mixture of different-sized colloidal particles are extremely interesting for application in metamaterials (*9, 10*). For example, providing that smaller colloidal particles are made of conductive material, the colloidal ring would represent a distributed split-ring resonator, with the electrical scheme shown in Figure 15(d). Here, the capacitor C is formed of the two conductive surfaces of the neighbouring smaller colloidal spheres within the Saturn ring, whereas the inductance L is formed of the small conductive colloidal particles. A series of conductive colloidal particles trapped into the ring, therefore, represent a distributed LC circuit. An estimate shows that for the 5 μm diameter of the colloidal ring and 50 nm diameter of the smaller colloidal particles, the resonant frequency of the distributed resonant circuit is of the order of 15 THz.

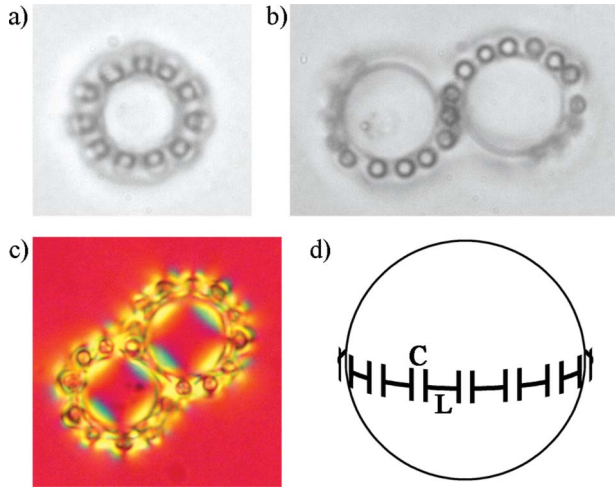

Figure 15. Hierarchical superstructures in a mixture of small and large colloidal particles in 4-cyano-4-n-pentylbiphenyl nematic liquid crystal. The cells are homeotropic. (a) Colloidal microsphere with smaller colloidal particles filling the Saturn ring around it. (b) Figure of eight defect ring entangling two microspheres is half-filled with smaller microspheres. (c) Birefringence image of fully filled figure of eight defect ring. (d) 'Electric scheme' of a split-ring resonator wrapped around a larger colloidal microsphere.

8. Conclusions

The aim of this contribution was to give a brief and simplified overview of the rapidly evolving field of nematic colloids. Within only a couple of years, a development from simple one-dimensional colloidal structures to complex two-dimensional crystals, entangled structures and hierarchical superstructures can be seen, which illustrates the richness of this field. There are several directions which can be explored in the future. For example, dispersions of colloidal particles of different sizes and nanoparticles could lead to new superstructures, which might be of great interest for photonic materials and metamaterials. Complex colloidal photonic structures, formed by different colloidal particles in two-dimensions, could lead to interesting applications for photonics, such as light-guiding devices and light switching elements in photonic structures.

Acknowledgement

First of all, I would like to thank Miha Škarabot for his valuable contribution to this work. I would also like to thank Miha Ravnik, Slobodan Žumer, Uroš Tkalec, Igor Poberaj, Dušan Babič, Natan Osterman, Andriy Nych, Ulyana Ognysta and Vassili Nazarenko.

References

(1) Grier, D.G. *Nature* **2003**, *424*, 810–816.
(2) Chiou, P.Yu.; Ohta, A.T.; Wu, M.C. *Nature* **2005**, *436*, 370–372.
(3) MacDonald, M.P.; Spalding, G.C.; Dholakia, K. *Nature* **2003**, *426*, 421–424.
(4) Psaltis, D.; Quake, S.R.; Yang, C. *Nature* **2006**, *442*, 381–386.
(5) Aoki, A.; Aoki, K.; Miyazaki, H.T.; Hirayama, H.; Inoshita, K.; Baba, T.; Sakoda, K.; Shinya, N.; Aoyagi, Y. *Nat. Mater.* **2003**, *2*, 117–121.
(6) van Blaaderen, A.; Ruel, R.; Wiltzius, P. *Nature* **1997**, *385*, 321–324.
(7) Joannopoulos, J.D.; Villeneuve, P.R.; Fan, S. *Nature* **1997**, *386*, 143–149.
(8) Vlasov, Y.A.; Bo, X.-Z.; Sturm, J.C.; Norris, D.J. *Nature* **2001**, *414*, 289–293.
(9) Veselago, V.G. *Sov. Phys. Usp.* **1968**, *10*, 509–513.
(10) Pendry, J.B. *Phys. Rev. Lett*. **2000**, *85*, 3966–3969.
(11) Hynninen, A.P.; Thijssen, J.H.J.; Vermolen, E.C.M.; Dijkstra, M.; van Blaaderen, A. *Nat. Mater.* **2007**, *6*, 202–205.
(12) Poulin, P.; Raghunathan, V.A.; Richetti, P.; Roux, D. *J. Physique* **1994**, *4*, 1557–1569.
(13) Poulin, P.; Stark, H.; Lubensky, T.C.; Weitz, D.A. *Science* **1997**, *275*, 1770–1773.
(14) Erb, R.M.; Son, H.S.; Samanta, B.; Rotello, V.M.; Yellen, B.B. *Nature* **2009**, *457*, 999–1002.
(15) Cladis, P.E.; Pieranski, P. *C. R. Acad. Sci.* **1971**, *273*, 275–277.
(16) de Gennes, P.G.; Prost, J. *The Physics of Liquid Crystals*, 2nd edition; Oxford Science Publications: Oxford, 1993.
(17) Ajdari, A.; Duplantier, D.; Hone, D.; Peliti, L.; Prost, J. *J. Physique* **1992**, *2*, 487–492.
(18) Stark, H. *Phys. Rep*. **2001**, *351*, 387.
(19) Ramaswamy, S.; Nityananda, R.; Raghunathan, V.A.; Prost, J. *Mol. Cryst. Liq. Cryst.* **1996**, *288*, 175–180.
(20) Raghunthan, V.A.; Richetti, P.; Roux, D.; Nallet, F.; Sood, A.K. *Mol. Cryst. Liq. Cryst*. **1996**, *288*, 181–187.
(21) Kuksenok, O.V.; Ruhwandl, R.W.; Shiyanovskii, S.V.; Terentjev, E.M. *Phys. Rev. E* **1996**, *54*, 5198–5205.
(22) Ruhwandl, R.W.; Terentjev, E.M. *Phys. Rev. E* **1997**, *55*, 2958–2961.
(23) Lubensky, T.C.; Pettey, D.; Currier, N.; Stark, H. *Phys. Rev. E* **1998**, *57*, 610–625.
(24) Pergamenshchik, V.M.; Uzunova, V.A. *Phys. Rev. E* **2009**, *79*, 021704–1–10.
(25) Kleman, M.; Lavrentovich, O.D. *Phil. Mag*. **2006**, *86*, 4117–4137.
(26) Yuedong, N.G.; Abbott, N.L. *Phys. Rev. Lett*. **2000**, *85*, 4719–4722.
(27) Stark, H. *Phys. Rev. E* **2002**, *66*, 032701–1–1.
(28) Mondain-Monval, O.; Dedieu, J.C.; Gulik-Krzywicki, T.; Poulin, P. *Eur. Phys. J. B* **1999**, *12*, 167–170.
(29) Terentjev, E.M. *Phys. Rev. E* **1995**, *51*, 1330–1337.
(30) Loudet, J.C.; Mondain-Monval, O.; Poulin, P. *Eur. Phys. J. E* **2002**, *7*, 205–208.
(31) Voeltz, C.; Maeda, Y.; Tabe, Y.; Yokoyama, H. *Phys. Rev. Lett.* **2006**, *97*, 227801–1–4.
(32) Škarabot, M.; Ravnik, M.; Žumer, S.; Tkalec, U.; Poberaj, I.; Babič, D.; Osterman, N.; Muševič, I. *Phys. Rev. E* **2008**, *77*, 031705–1–8.
(33) Ashkin, A. *Phys. Rev. Lett.* **1970**, *24*, 156–159.
(34) Prasad, P.N. *Introduction to Biophotonics*; John Wiley: Hoboken, NJ, 2003.
(35) Yada, M.; Yamamoto, J.; Yokoyama, H. *Langmuir* **2002**, *18*, 7436–7440.
(36) Yada, M.; Yamamoto, J.; Yokoyama, H. *Phys. Rev. Lett.* **2004**, *92*, 185501–1–4.
(37) Smalyukh, I.I.; Kuzmin, A.N.; Kachynski, A.V.; Prasad, P.N.; Lavrentovich, O.D. *Appl. Phys. Lett.* **2005**, *86*, 021913–1–3.
(38) Smalyukh, I.I.; Lavrentovich, O.D.; Kuzmin, A.N.; Kachynski, A.V.; Prasad, P.N. *Phys. Rev. Lett.* **2005**, *95*, 157801–1–4.
(39) Takahashi, K.; Ichikawa, M.; Kimura, Y. *Phys. Rev. E* **2008**, *77*, 020703(R)–1–4.
(40) Juodkazis, S.; Iwashita, M.; Takahashi, T.; Matsuo, S.; Misawa, H. *Appl. Phys. Lett*. **1999**, *74*, 3627–3629.
(41) Juodkazis, S.; Matsuo, S.; Murazawa, N.; Hasegawa, I.; Misawa, H. *Appl. Phys. Lett*. **2003**, *82*, 4657–4659.
(42) Iwashita, Y.; Tanaka, H. *Phys. Rev. Lett.* **2003**, *90*, 045501–1–4.
(43) Pattanaporkratana, A.; Park, C.S.; Maclennan, J.E.; Clark, N.A. *Ferroelectrics* **2004**, *310*, 131–136.
(44) Wood, T.A.; Gleeson, H.F.; Dickinson, M.R.; Wright, A.J. *Appl. Phys. Lett.* **2004**, *84*, 4292–4294.
(45) Hotta, J.; Masuhara, H. *Appl. Phys. Lett.* **1997**, *71*, 2085–2087.
(46) Muševič, I.; Škarabot, M.; Babič, D.; Osterman, N.; Poberaj, I.; Nazarenko, V.; Nych, A. *Phys. Rev. Lett*. **2004**, *93*, 187801–1–4.
(47) Škarabot, M.; Ravnik, M.; Babič, D.; Osterman, N.; Poberaj, I.; Žumer, S.; Muševič, I.; Nych, A.; Ognysta, U.; Nazarenko, V. *Phys. Rev. E* **2006**, *73*, 021705–1–10.
(48) Loudet, J.C.; Hanusse, P.; Poulin, P. *Science* **2004**, *306*, 1525.
(49) Poulin, P.; Weitz, D.A. *Phys. Rev. E* **1998**, *57*, 626–637.
(50) Nych, A.B.; Ognysta, U.M.; Pergamenshchik, V.M.; Lev, B.I.; Nazarenko, V.G.; Muševič, I.; Škarabot, M.; Lavrentovich, O.D. *Phys. Rev. Lett*. **2007**, *98*, 057801–1–4.
(51) Smalyukh, I.I.; Chernyshuk, S.; Lev, B.I.; Ognysta, U.; Nazarenko, V.G.; Lavrentovich, O.D. *Phys. Rev. Lett.* **2004**, *93*, 117801–1–4.
(52) Zapotocky, M.; Ramos, L.; Poulin, P.; Lubensky, T.C.; Weitz, D.A. *Science* **1999**, *283*, 209–212.
(53) Meeker, S.P.; Poon, W.C.K.; Crain, J.; Terentjev, E.M. *Phys. Rev. E* **2000**, *61*, R6083–6086.
(54) Petrov, P.G.; Terentjev, E.M. *Langmuir* **2001**, *17*, 2942–2949.
(55) Muševič, I.; Škarabot, M.; Tkalec, U.; Ravnik, M.; Žumer, S. *Science* **2006**, *313*, 954–958.
(56) Škarabot, M.; Ravnik, M.; Žumer, S.; Tkalec, U.; Poberaj, I.; Babič, D.; Osterman, N.; Muševič, I. *Phys. Rev. E* **2008**, *77*, 031705–1–8.
(57) Škarabot, M.; Ravnik, M.; Žumer, S.; Tkalec, U.; Poberaj, I.; Babič, D.; Osterman, N.; Muševič, I. *Phys. Rev. E* **2007**, *76*, 051406–1–8.
(58) Poulin, P.; Cabuil, V.; Weitz, D.A. *Phys. Rev. Lett.* **1997**, *79*, 4862–4865.

(59) Loudet, J.C.; Poulin, P. *Phys. Rev. Lett.* **2001**, *87*, 165503–1–4.
(60) Noel, C.M.; Bossis, G.; Chaze, A.-M.; Giulieri, F.; Lacis, S. *Phys. Rev. Lett*. **2006**, *96*, 217801–1–4.
(61) Kotar, J.; Vilfan, M.; Osterman, N.; Babič, D.; Čopič, M.; Poberaj, I. *Phys. Rev. Lett.* **2006**, *96*, 207801–1–4.
(62) Ognysta, U.; Nych, A.; Nazarenko, V.; Muševič, I.; Škarabot, M.; Ravnik, M.; Žumer, S.; Poberaj, I.; Babič, D. *Phys. Rev. Lett*. **2008**, *100*, 217803–1–4.
(63) Guzman, O.; Kim, E.B.; Grollau, S.; Abbott, N.L.; de Pablo, J.J. *Phys. Rev. Lett.* **2003**, *91*, 2355207–1–4.
(64) Žumer, S. Plenary Talk at the 21st International Liquid Crystal Conference, Keystone, Colorado, July 2–7, 2006.
(65) Araki, T.; Tanaka, H. *Phys. Rev. Lett.* **2006**, *97*, 127801–1–4.
(66) Ravnik, M.; Škarabot, M.; Žumer, S.; Tkalec, U.; Poberaj, I.; Babič, D.; Osterman, N.; Muševič, I. *Phys. Rev. Lett*. **2007**, *99*, 247801–1–4.
(67) Antypov, D.; Cleaver, D.J. *J. Phys. Condens. Matter* **2004**, *16*, S1887–1900.
(68) Pires, D.; Fleury, J.-B.; Galerne, Y. *Phys. Rev. Lett.* **2007**, *98*, 247801–1–4.
(69) Grollau, S.; Abbot, N.L.; de Pablo, J.J. *Phys. Rev. E* **2003**, *67*, 051703–1–9.
(70) Škarabot, M.; Ravnik, M.; Žumer, S.; Tkalec, U.; Poberaj, I.; Babič, D.; Muševič, I. *Phys. Rev. E* **2008**, *77*, 061706–1–4.